

---

# A space of goals: the cognitive geometry of informationally bounded agents

Karen Archer<sup>1,\*</sup>, Nicola Catenacci Volpi<sup>1</sup>, Franziska Bröker<sup>2,3</sup>, Daniel Polani<sup>1</sup>

1 Adaptive Systems Group, Department of Computer Science, University of Hertfordshire, Hatfield, United Kingdom

2 Gatsby Computational Neuroscience Unit, University College London, London, United Kingdom

3 Max Planck Institute for Biological Cybernetics, Tübingen, Germany

\* karen.archer@gmail.com

## Abstract

Traditionally, Euclidean geometry is treated by scientists as a priori and objective. However, when we take the position of an agent, the problem of selecting a best route should also factor in the abilities of the agent, its embodiment and particularly its cognitive effort. In this paper we consider geometry in terms of travel between states within a world by incorporating information processing costs with the appropriate spatial distances. This induces a geometry that increasingly differs from the original geometry of the given world, as information costs become increasingly important. We visualize this “*cognitive geometry*” by projecting it onto 2- and 3-dimensional spaces showing distinct distortions reflecting the emergence of epistemic and information-saving strategies as well as pivot states. The analogies between traditional cost-based geometries and those induced by additional informational costs invite a generalization of the traditional notion of geodesics as cheapest routes towards the notion of *infodesics*. Crucially, the concept of infodesics approximates the usual geometric property that, travelling from a start to a goal along a geodesic, not only the goal, but all intermediate points are equally visited at optimal cost from the start.

**Keywords:** information-regularized MDPs, decision sequences, constrained information processing, geometry, cognitive load

## Introduction

Traditional Reinforcement Learning (RL) [31] is often centred around agents moving towards a specific goal. The problem of designing agents that can address multiple concurrent objectives at the same time has recently become of pivotal importance in RL [16, 40]. While start and goal states are part of the same world, the resulting policies are often merely collected in the form of a “catalogue” for the different start/goal combinations. Here we wish to start from a fundamentally geometric position: we posit that in a world where the agent incurs movement costs for each action (negative rewards only), and trajectories implement directed shortest routes between a start and a goal point, these become a part of a geometry, in the case of continuous deterministic trajectories, a so-called *Finsler geometry* [39]. Here they are no longer a catalogue of unrelated policies and traces of agent movement through the world, but in their totality form a space with a pervasive overall structure. Such a structure puts these different trajectories and the policies used to achieve them in relation with each other and allows us to systematically draw conclusions about their commonalities, what the space between these tasks looks like and how to switch between tasks or trajectories, and,

---

finally, of course, how to generalise solutions. The best-known form of such a structure is Euclidean geometry.

Classical Euclidean geometry is often considered as a “static” concept. However, one can alternatively interpret it also as the entirety of locations of a set under consideration, together with the straight lines defining the shortest routes of travel between these locations, and the associated directions determined by such straight lines. This concept generalises into Riemannian geometry by replacing straight lines with geodesics which represent a kind of consistent directionality on a manifold. Riemannian geometry still respects the symmetry of distance between locations. One can generalise this to direction-dependent routes in terms of Finsler geometry where such distances are no longer symmetric between two given points; this models, for instance, non-reversible energy expenditure, altitude traversal, or ease of terrain. This can be elegantly expressed as RL problems which carry only positive cost (or negative reward, our convention throughout the paper).

Work in the last decade has begun to include not only traditional performance rewards into such RL problems, but also a cost for the cognitive processing to operate a given policy, measured in terms of information-theoretic functionals [22, 30]. In the present paper, we are interested in the geometries emerging from the incorporation of such informational cognitive costs [2]. Such generalised geometries with their directional routes represent the totality of tasks that one may consider solving and thus offer a much richer and more robust representation of problem solving. Taken together with a cognitive cost we can additionally ask how such a geometry would ideally be organized and represented in an informationally limited agent. We note that this perspective, while carrying some similarity to the questions of transfer learning [33], is still markedly distinct. No symmetry or equivariance is implied, only operational and cognitive distances (costs) and their associated policies — in particular, there is no reason to assume that one type of strategy carries over to another region.

We generally consider geometry in terms of locations (points) and optimal routes from a start location to another. Such routes are characterised by a *distance* (in our RL-based convention, negative cumulated rewards) and *direction* (which we formalise later). In two-dimensional continuous Euclidean space, the optimal routes consist of straight lines which also form shortest paths between two points. On a sphere, optimal routes lie on grand circles connecting two points; they can be naturally extended beyond these points to full grand circles. These form *geodesics* which no longer necessarily constitute shortest routes. Instead, they are *direction-preserving curves*, a generalisation of the Euclidean straight line [28].

In order to define a concept of direction we use the above reinterpretation of the given geometry as a family of RL problems. Consider our agent starting at a given point and proceeding unchanged to “move in one direction”, a fixed given behaviour; we now ask which goals (in addition to the original one) will be optimally reached following this fixed behaviour. In the case where cognitive costs incorporate the cost of processing information we will also speak of *infodesics*. Constraining information processing can thus trade in nominally shorter but more complicated routes against longer, but simpler and safer ones [14, 30], which effectively imposes a distortion on the geometry of a task space.

To investigate this further, we define *Decision Information* to quantify the amount of information processed by an agent to execute a policy to navigate from a starting location to the goal state. Here, we use an information-theoretic free energy principle [7, 14, 19, 22, 30, 35], which induces a notion of informational distance and endows the decision-making problem with a geometrical interpretation.

*InfoRL* [30] is a measure which, like Decision Information, focuses on decisions and ignores the surprise registered by the environment regarding each action selection. The information cost in InfoRL is the Kullback-Leibler divergence between the optimised policy and a prior comprised of uniformly distributed actions. Larsson et al. [14] extends the work on InfoRL [30] to study the possibility of finding an optimal prior action distribution which minimises the information cost across all states on average.

Finally, Mutual Information Regularisation [9] quantifies the trade-off between information and value as a regularising signal to facilitate exploration and increase robustness in reinforcement learning. Like Decision Information in the present paper, it employs a marginal action distribution in the information measure [15, see (4)].

We now introduce our formalism. After describing the simulations implemented, we present and discuss the results with suggestions for future avenues of research.

## Methods

We seek to model an agent’s behaviour and the trade-off between information processing and performance. Concretely, here we model discrete gridworlds as a discrete Markov Decision Process (MDP). Critically, here we interpret action choice in a state as the discrete analogue of geometrical “direction” selection in that state.

### Markov Decision Process (MDP) Framework

We model the system interactions between the environment and an agent ensuing from a sequence of decisions at discrete time steps for  $t \in 0, \dots, T$  using an undiscounted MDP [29] defined by the tuple  $\langle \mathcal{S}, \mathcal{A}, r, P \rangle$ . At time  $t$ , the state of the environment is  $s_t \in \mathcal{S}$  ( $\mathcal{S}$  denoting the set of states with random variable  $S \in \mathcal{S}$ , and similarly for the set of actions  $\mathcal{A}$ , with random variable  $A \in \mathcal{A}$ ). The policy  $\pi(a_t|s_t)$  denotes the conditional probability distribution  $\Pr\{A = a_t|S = s_t\}$  which defines a stochastic choice of actions in each state  $s_t$  at time  $t$ . Note that, as appropriate, we will drop the temporal index  $t$  of  $s$  and  $a$  to emphasise that the policy, transition probability and reward function do not depend on time, but only on the states involved.

The dynamics of the MDP is modelled using state-action probability matrices  $P_{ss'}^a$  which define the distribution of the successor state ( $s_{t+1}$  is denoted as  $s'$  where unambiguous, with random variable  $S' \in \mathcal{S}$ ) given a current state and action, according to  $P_{ss'}^a \equiv p(s'|s, a) \doteq \Pr\{S' = s'|S = s, A = a\}$ . As a consequence of each action  $a_t \in \mathcal{A}$ , the agent receives a reward in the subsequent time step,  $r(s', s, a)$ .

When following a value optimal policy  $\pi_v^*$ , the agent selects a sequence of actions with the aim of maximising the expected future cumulated rewards, also referred to as the *return*. We only consider cost-only MDPs here, that is, all rewards  $r$  incurred in transient states are negative,  $r \in (-\infty, 0)$ . Goal states, denoted by  $g \in \mathcal{S}$ , are absorbing, i.e.  $p(s' = g|s = g, \cdot) = 1$ , and once the agent reaches a goal, no further (negative) rewards are incurred. i.e.  $r(g, \cdot, \cdot) = 0$ .

We model state distance by each single transition receiving a reward of  $-1$ . The value function  $V^\pi(s)$  represents the expected return of an agent when starting in a given state  $s$  and following policy  $\pi$  [31]. We here interpret the optimal value function  $V^*$  as the negative distance between the agent’s position  $s$  and a given goal state. Equation (1) shows the value function expressed in the form of a recursive Bellman equation.

$$V^\pi(s) = \sum_a \pi(a|s) \sum_{s'} p(s'|s, a) [r(s', s, a) + V^\pi(s')]. \quad (1)$$

We assume throughout that the expected return exists and is finite (in particular, that the probability for trajectories generated by optimal policies to terminate at a goal state is one).

### Information Processed in a Decision Sequence

To treat cognitive costs, we formalise the information processed in a sequence of decisions [35]. Compared to the original definition of Information-to-go, here we drop the conditioning on actions and condition only on the current state because we want to compare the Information-to-go based on states only. We also extract only the component which exclusively impacts the decision complexity, as we are only interested

in the information cost for the decision-maker. Thus we define *Decision Information* for a policy  $\pi$  as the decision cost of an agent following  $\pi$  for future trajectories starting in  $s_t$ , as per

$$\mathfrak{S}_D^\pi(s) \doteq \mathbb{E}_{p(a,s'|s)} \left[ \log \frac{\pi(a|s)}{\hat{p}(a)} + \mathfrak{S}_D^\pi(s') \right]. \quad (2)$$

The prior  $\hat{p}(\cdot)$  encodes all information known a priori about the action process and we assume policy-consistent factorised action distributions  $\hat{p}(a_{t+1}), \hat{p}(a_{t+2}), \dots$  (3) and state distributions  $\hat{p}(s_{t+1}), \hat{p}(s_{t+2}), \dots$  [35]. In the literature,  $\hat{p}(s)$  is typically distributed according to a uniform distribution [14, 30, 35]. However, using uniform distributions as prior has the problem that the distribution fails to take into account that some states are unlikely to be visited, except for rare trajectories, while others (e.g. close to a goal) will concentrate far more probability mass. We therefore work with a *live distribution* on the states  $s$ ; this is the probability of finding the agent at this particular state at some random time of carrying out its policy  $\pi$  if it originally started its trajectory uniformly somewhere in the state space, with  $s \in \mathcal{S} \setminus g$ .

From this, the marginal distribution of actions  $\hat{p}(a; \pi)$ , calculated using (3), is computed which reflects the agents' future choice of actions weighted by the probability of having to select them:

$$\hat{p}(a; \pi) = \sum_{s \in \mathcal{S}} \pi(a|s) \hat{p}(s; \pi). \quad (3)$$

## Constraining Information Processing

The traditional MDP framework assumes the agent is able to access and process all information necessary for an optimal decision. However, when information processing resources are scarce, we want the agent to prioritise the processing of essential information only. This can be achieved, for instance, by compressing state information as much as possible without compromising performance [27]. Information-theoretically, one can consider the sequence of states in the agent's trajectory as input and the respective actions taken as output; in analogy to rate-distortion theory [5], one then seeks the lowest information rate required to reach a certain value.

Formally, we seek a solution to the following constrained optimisation problem, with the desired information rate  $\tilde{\mathfrak{S}}_D(s)$  determining the trade-off between information processing and performance:

$$\max_{\pi(a|s)} V^\pi(s) \text{ s.t. } \mathfrak{S}_D^\pi(s) = \tilde{\mathfrak{S}}_D(s). \quad (4)$$

For optimization, we write this as an unconstrained Lagrangian (5), with the Lagrangian multiplier  $\beta$  for the information rate constraint  $\tilde{\mathfrak{S}}_D$  and  $\lambda$  for the normalisation of the policy:

$$\mathcal{L}^\pi(s; \beta, \lambda) \doteq \frac{1}{\beta} \mathfrak{S}_D^\pi(s) - V^\pi(s) + \lambda \left( 1 - \sum_a \pi(a|s) \right). \quad (5)$$

Note that, in principle one might choose a different Decision Information threshold  $\tilde{\mathfrak{S}}_D(s)$  for each state as per (4). However, since it is not obvious how to choose per-state thresholds consistently [3], we instead choose the same  $\beta$  for each state, which defines a different threshold for every state  $\tilde{\mathfrak{S}}_D(s)$  in a natural way. In practice, this is achieved by a double iteration combining the Bellman equation with the Blahut-Arimoto algorithm [1], see [14] and the algorithm detailed in the Supplementary Material. Minimising the Lagrangian when  $\beta$  is very small yields a policy  $\pi$  where Decision Information is the dominant term (5) and the agent aims to minimize information processing at the expense of increasing distance cost.

## Free energy

We here define free energy as the Lagrangian of the value function constrained by Decision Information (2). Free energy optimisation then trades off expected utility against the cost of the information processing required to execute the behaviour policy [14, 23]. In our cost-only MDPs  $\mathfrak{S}_D^\pi \geq 0$  and  $V^\pi \leq 0$ , thus their free energy is always nonnegative. The trade-off parameter  $\beta$  will be strictly non-zero.

$$\mathcal{F}^\pi(s; \beta) \doteq \frac{1}{\beta} \mathfrak{S}_D^\pi(s) - V^\pi(s). \quad (6)$$

From value (1) and Decision Information (2), free energy inherits the form of a Bellman equation. The optimal free energy  $\mathcal{F}^*(s; \beta)$  is taken at the fixed point of equation (7) [14] using the corresponding free energy optimal policy  $\pi_{\mathcal{F}}^*$ . The free energy is additive for the whole sequence of decisions, this monotonicity is crucial for us to be able to use free energy as a distance measure.

$$\mathcal{F}^\pi(s; \beta) = \sum_a \pi(a|s) \sum_{s'} p(s'|s, a) \left[ \frac{1}{\beta} \log \frac{\pi(a|s)}{\hat{p}(a)} - r(s', s, a) + \mathcal{F}^\pi(s') \right]. \quad (7)$$

For the remainder of this paper, unless stated otherwise, by ‘‘optimal policy’’ we mean  $\pi_{\mathcal{F}}^*$ . For ease of notation, we drop the superscript  $\pi$  for the value function and free energy if the agent follows the respective optimal policy to the specified goal state  $g$ .

## Geodesics and Infodesics

Since moving in one direction with  $\pi$  may incur a different cost from moving in the reverse direction, the distance measured by  $-V_g^\pi(s)$  is asymmetric in general and thus acts as a quasimetric. Cost-only deterministic MDPs are, in terms of distance, equivalent to directed graphs with nonnegatively weighted edges. Therefore, we can write the triangle inequality as  $V_{s'}(s) + V_g(s') \leq V_g(s)$ , for all  $s, s', g \in \mathcal{S}$ , where  $s'$  is some arbitrarily chosen intermediate state. Armed with these observations, we now define a *value geodesic* from  $s$  to  $g$  to be a sequence  $\tau_{s \rightarrow g} = \langle s_0 = s, s_1, s_2, \dots, s_T = g \rangle$ ,  $s_i \in \mathcal{S}$  such that all elements of the sequence turn a generalisation of the triangle inequality into an equality, i.e.

$$V_g(s) = \sum_{i=0}^{T-1} V_{s_{i+1}}(s_i) \text{ with } s_i \in \tau_{s \rightarrow g}. \quad (8)$$

Note that not all states on a trajectory traveled by an optimal policy need to be part of the value geodesic. The states on such a value geodesic each lie on a shortest path from the current state  $s$  to the goal. This has an important consequence: each state on this sequence can be considered a potential alternative goal that can be reached optimally from  $s$  while en route to  $g$ . It means that benefits from reaching these intermediate goals can be ‘‘scooped up’’ on the way to the main goal. Within this sequence, the value is strictly monotonically increasing, i.e.  $V_g(s_n) < V_g(s_m)$  for  $n < m$ . It is important to reiterate that in the context of interim goals, the agent might follow a different optimal policy for each separate portion of a trajectory. Since information processing cost will play a major role later, this observation is significant because policies vary in terms of their informational processing costs.

Motivated by this concept of geodesics, and taking inspiration from differential geometry, we propose an analogous concept in our space where distances are determined partially or completely by an information-theoretic component. We term this concept *infodesics*. We will first consider *pure infodesics* as stochastic trajectories through the space composed of states that can be visited by the agent using no state information, i.e. with action selection being independent of state. The intuition is that, as with traditional geodesics, following infodesics one obtains all interim states optimally at no extra decision cost after choosing the initial direction (i.e. policy in our perspective).

We define a *cost infodesic* as a value geodesic where the value function  $V$  has been replaced by the free energy function  $\mathcal{F}$ . A cost infodesic in a discrete MDP is thus a sequence  $\psi_{s_0 \rightarrow g} = \langle s_0 = s, s_1, \dots, s_T = g \rangle$ ,  $s_i \in \mathcal{S}$  such that, again, all elements of the sequence turn the generalisation of the triangle inequality for free energy over multiple steps into an equality (9). Note that the value of  $\mathcal{F}_g$  is strictly monotonically decreasing, i.e.  $\mathcal{F}_g(s_n) > \mathcal{F}_g(s_m)$  for  $n < m$ . Following an optimal policy to reach goal state  $g$ , the agent is able to follow a planned direction, only processing at a given information level. Formally, we demand for a cost infodesic that:

$$\mathcal{F}_g(s) = \sum_{i=0}^{T-1} \mathcal{F}_{s_{i+1}}(s_i) \text{ with } s_i \in \psi_{s_0 \rightarrow g} \text{ by abuse of notation.} \quad (9)$$

## Numerical Simulations

We conducted simulations of a navigational task in a 2D gridworld modelled as a cost-only MDP with a discrete and finite state space. While considering with deterministic transitions, the framework generalises to the non-deterministic case. Details of the algorithm and the code repository are included in the supporting material. Starting from an initial state, at each time step the agent selects an action representing a move in the given neighbourhood: in Manhattan, with action set  $\mathcal{A} : \{\uparrow, \leftarrow, \downarrow, \rightarrow\}$ , in Moore, with action set  $\mathcal{A} : \{\uparrow, \nearrow, \leftarrow, \swarrow, \downarrow, \searrow, \rightarrow, \nearrow\}$ . If the agent bumps into a wall, the agent does not move but still receives a reward of  $-1$ .

To model cognitive distances, we compute free energies  $\mathcal{F}_{s_j}(s_i)$  between all combinations of pairs of states,  $s_i, s_j \in \mathcal{S}$ , creating an  $n \times n$  pair-wise matrix  $D$ , with elements  $d_{ij} \doteq \mathcal{F}_{s_j}(s_i)$ . In order to visualise these distances in 2D/3D Euclidean space,  $D$  is symmetricised into  $D^{\text{sym}}$  by taking the average of the reciprocal trajectories, i.e.  $d_{ij}^{\text{sym}} \doteq \frac{d_{ij} + d_{ji}}{2}$ , hence

$$D^{\text{sym}} \doteq \frac{D + D^{\top}}{2}. \quad (10)$$

For visualisation, we used a non-linear mapping algorithm, Multidimensional Scaling (MDS) [13], which, given the symmetrical pairwise distances between points in a set, projects each point onto an  $N$ -dimensional space such that the distances between objects are preserved as much as possible. We use the Scikit-learn MDS algorithm [24] to qualitatively assess the distance-related aspects of geometry imposed by the trade-off between value (grid distance) and information.

To investigate the analogy with traditional geodesics, discrete infodesics were identified by performing an exhaustive search over sequences formed by every non-repeating combination of sequences of 3, 4 or 5 states. The states in this sequence were taken to be interim goals; free energy and respective optimal policies were calculated for each subtrajectory within the sequence. Since in our setup, strict infodesics may end up not containing any intermediate states, we relaxed the generalised triangle inequality requirement for the infodesic and defined an  $\varepsilon$ -*infodesic* such that the normalised difference between the sum of the free energy for the trajectory with interim goals and the total, single-goal free energy  $\mathcal{F}_{s_T}(s_0)$ , is less than  $\varepsilon$ , with  $0 < \varepsilon \ll 1$  via (11). As we will show later, this normalised difference can become negative, as is the case, discussed below, when it is advantageous to use multiple policies.

$$\frac{[\sum_{i=0}^{T-1} \mathcal{F}_{s_{i+1}}(s_i)] - \mathcal{F}_{s_T}(s_0)}{\mathcal{F}_{s_T}(s_0)} < \varepsilon. \quad (11)$$

## Results

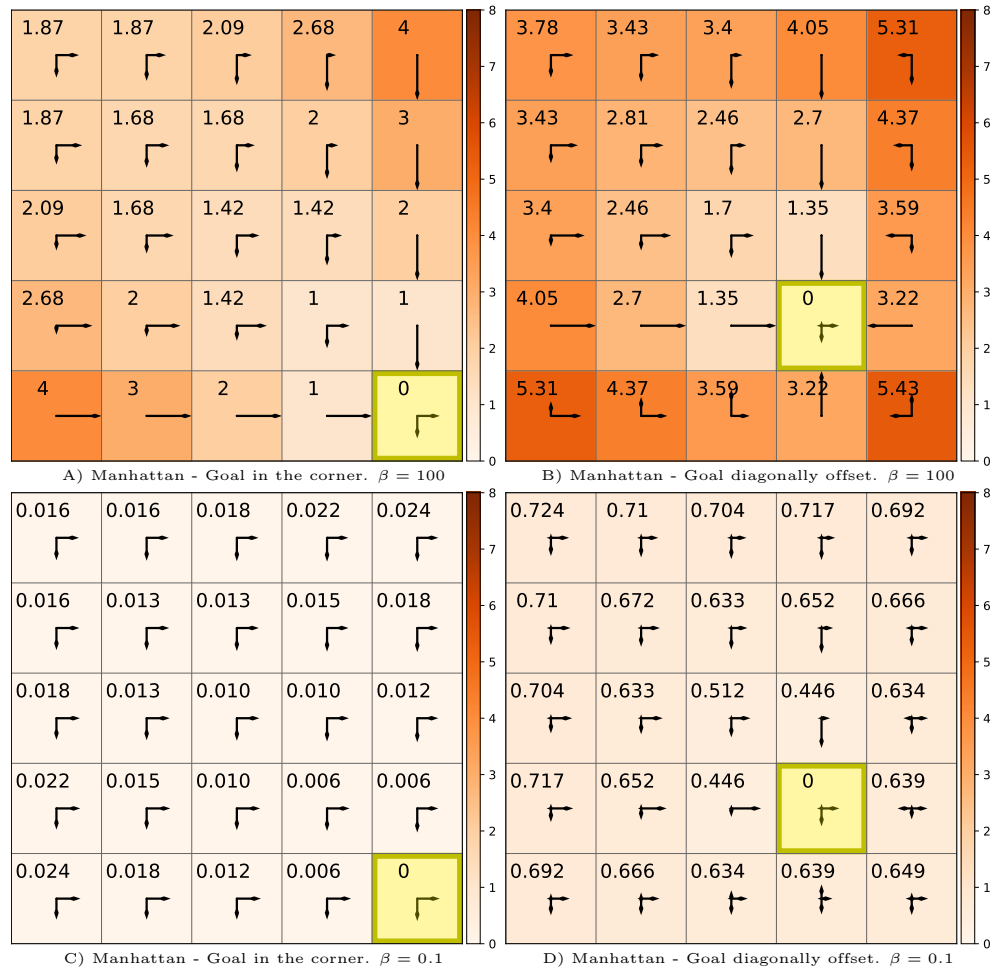
We now present geometries that emerge under optimal policies, elucidating the nature of Decision Information, and then proceed to demonstrate the trade-off between performance and cognitive burden, showing how constraints on information processing

impact the geometry of the gridworld. In what follows, the optimal policy  $\pi_{\mathcal{F}}^*$  is that which minimises the free energy, not to be confused with reward-maximising behaviour  $\pi_{\mathcal{V}}^*$  where the agent minimises the number of steps taken to reach the goal.

## Decision Information

Fig. 1 displays heat maps for a  $5 \times 5$  gridworld with Manhattan actions. Each square in the grid is a state, with goal states denoted in yellow. The value of Decision Information, in bits, for the free energy optimal policy, is indicated by the background colour in transient (non-goal) states, and given by its numerical annotation. The arrows represent the policy for the agent acting in that square. The length of the arrows are proportional to the value of the conditional probability  $\pi(a|s)$ , with the action  $a$  indicated by the arrow direction. The policy within the goal represents the action marginal  $\hat{p}(a; \pi)$ , which enables convenient comparison with the denominator in (2) when interpreting Decision Information.

**Figure 1. Decision Information heat map** in a  $5 \times 5$  gridworld with  $\mathcal{A} : \{\uparrow, \leftarrow, \downarrow, \rightarrow\}$ . Annotated values show  $\mathfrak{S}_D^\pi(s)$  in bits. The policy presented is optimal with respect to free energy, i.e.  $\pi_{\mathcal{F}}^* = \arg \min_{\pi} \mathcal{F}(s; \beta)$ . The arrow lengths are proportional to the conditional probability  $\pi(a|s)$  in the indicated direction, for convenience  $\hat{p}(a)$  is shown in the yellow goal state. **Reward-maximising behaviour ( $\beta = 100$ ):** In **A** the goal is in the corner and in **B** the goal is on the diagonal between the corner and the middle. **Behaviour where information processing is constrained ( $\beta = 0.1$ ):** **C** the goal is in the corner and in **D** it is diagonally adjacent to the corner.



Decision Information computes the information processed for the *whole* sequence of decisions, and thus depends on the length of the sequence. This additivity is readily seen in Fig. 1A on the trajectory moving outwards from the goal along the lower edge, where each action adds one bit to the information processing cost and longer routes thus become informationally more expensive.

Referring to (2), we see that Decision Information increases when the alignment between the policy in a particular state and the marginalised action distribution  $\hat{p}(a; \pi)$  decreases. Fig. 1B shows Decision Information for a goal state in between the top left

corner and the middle of the grid. Starting from above or left of the goal, the agent is required to select actions which oppose the prevailing actions in the marginalised action distribution, causing a noticeable increase of Decision Information in these squares. For example, consider the Decision Information in the states adjacent to the goal:  $\mathfrak{I}_D^\pi = 3.22$  bits directly below the goal, in contrast to  $\mathfrak{I}_D^\pi = 1.35$  bits directly above the goal.

## Trade-off between Performance and Cognition

In minimising free energy, the trade-off parameter  $\beta$  (6) determines how parsimonious an agent is with respect to information processing. As  $\beta$  increases, minimising free energy cares less about information and more about performance, thus the resulting optimal policy requires more information to be processed. Executing the policy thus makes increasing use of information until the performance approaches the reward-optimal value  $V^*(s)$ , where the information processing cost reaches its maximum and the agent takes a shortest path ( $\beta > 100$  in our experiments).

Because agents are often required to act parsimoniously when processing information [8, 18, 25], we wish to understand the consequences of these constraints. As  $\beta$  decreases, the optimal policy with respect to free energy processes increasing less information, indicated by lower  $\mathfrak{I}_D^\pi(s)$  values (see Fig. 1C and D with  $\beta = 0.1$ ). In the limit of  $\beta \rightarrow 0$ , the agent is moving towards an open-loop policy which processes no information, therefore  $\mathfrak{I}_D^\pi \rightarrow 0$  and the policy approaches the marginal  $\hat{p}(a)$  (3).

Between the two extremes of value-optimal and open-loop behaviours, the policies are less state-specific, tolerating a more general strategy as in Fig. 1C with the goal in the corner. Here, by comparison with Fig. 1A, the distribution of actions applied in a particular state is notably more similar across all states.

## Cognitive Geometry

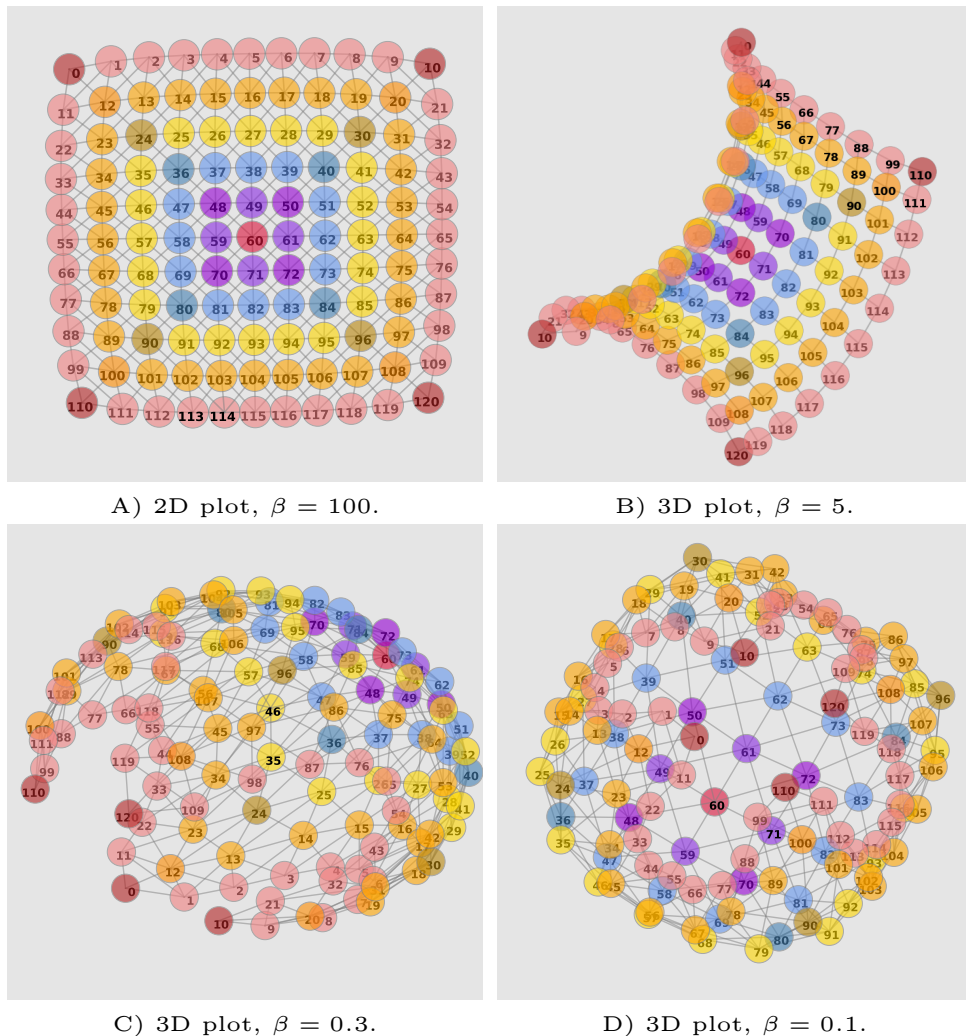
Cognitive geometry shapes the way agents represent the distance between states of the environment when information costs are taken into account. Fig. 2 presents two- and three- component MDS embeddings for the symmetrised free energy pairwise distances (10) in an  $11 \times 11$  gridworld with a Moore neighbourhood for different  $\beta$  values. If an agent behaves optimally with respect to value alone ( $\beta = 100$ ) then the cognitive geometry is simply the original Moore geometry, as indicated in Fig. 2A, and the underlying grid is prominently discernible.

The nodes in these and future graphs represent states which are numbered starting from zero to  $|\mathcal{S}|$  and increasing first along consecutive columns and then row-wise. The colours of the nodes distinguish between different categories of states, e.g. having different locations with respect to the centre and whether or not they lie on the diagonal. The edges between the nodes indicate possible one-step transitions between states via actions.

An agent can take repeated actions to move diagonally and also get additional guidance along the edges, as bumping into them incurs only a minor time penalty. Thus the wall acts as a guide or “funnel” buffering some wrong actions on the way to the corner goal. In contrast, to reach the middle goal, any wrong action is likely to move the agent away from the goal. Thus much more accurate control is required to reach precisely the middle goal compared to drifting into a corner. Since the informational cost of executing an optimal policy thus depends drastically on the nature of the goal, our distance, which takes this informational cost into account, will significantly distort the geometry of the gridworld as compared to a naive spatial map. When information processing is restricted via progressively lower  $\beta$  values, information processing becomes more expensive than the extra time cost for bumping into the wall, and policies which utilise the guiding property of the edges are increasingly preferred. Thus, states on the edges, even more so in the case of the corners, effectively become closer in terms of free energy distances, as if the spatial geometry were wrapped around a ball with the corners drawn together, see Fig. 2 C & D.



**Fig. 2. MDS visualisation of the cognitive geometry induced by free energy in a Moore  $11 \times 11$  gridworld.** As  $\beta$  decreases, the corners migrate towards each other and the topology morphs from a flat grid to a mesh wrapped over a ball. **A** At  $\beta = 100$ , the free energies approach the optimal value function  $V^*$ . With the reduction of  $\beta$ , **B**  $\beta = 5$ , **C**  $\beta = 0.3$  and **D**  $\beta = 0.1$ . As a result of the constrained information processing, the policy results in similar actions taken in multiple states, i.e. the agent moves in consistent directions across the grid. The routes to the corners and along the edges are more informationally efficient, with the effect that corners migrate towards each other, despite being farthest away from each other in the original grid distance.



## Cost Infodesics

We study cost infodesics in a  $7 \times 7$  Moore gridworld with three sets of examples order of decreasing values of  $\beta$ : reward-maximising behaviour, at  $\beta = 100$ ; limited information processing, at  $\beta = 0.07$ ; and near-minimal information processing, at  $\beta = 0.01$ . Figures 3, 4 and 5 present these infodesics as sequences of not necessarily contiguous interim states which are highlighted in green. Free energies of trajectories, i.e.  $\mathcal{F}_g(s_0)$  refer to the starting and goal states denoted by indices consistent with the state numbering of the sequence plot.

Fig. 3A displays the Decision Information and near value-optimal policy ( $\beta = 100$ ) obtained with the goal in the corner ( $S = \#6$ ). States on the diagonal between the goal and the opposite corner have lower Decision Information values. In these states, the distribution of actions is similar to the marginalised action distribution (displayed in the yellow goal state) and are thus informationally more efficient. The policy of states not on this diagonal favours actions which are either parallel with the diagonal or move the agent towards this diagonal. Fig. 3B shows the same policy, however the heat map and grid is now annotated with the values of the live state distribution  $\hat{p}(s; \pi)$ . This diagram shows that the probability mass of the state distribution is maximal at state  $S = \#12$  which is diagonally adjacent to the goal, with  $\hat{p}(S = \#12; \pi) \simeq 0.2$ . The next largest

concentration of probability mass is  $p(S = \#18; ) = 0.08$ , also on the diagonal. This demonstrates that the policy guides the agent towards the informationally efficient states on the diagonal en route to the goal.

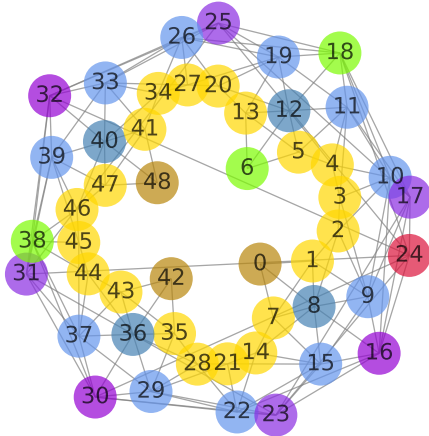
This sequence constitutes a cost infodesic  $s_0!_g = \#0; \#12; \#6$  starting from corner state  $s_0 = \#0$  and ending in another corner along the same edge ( $= \#6$ ). Its normalised free energy difference  $\frac{(F_{12}(0) + F_6(12)) - F_6(0)}{F_6(0)} = 0.0005$  in other words, practically respecting the equality (9); this is thus a near-pure infodesic.

Figure 3. Infodesic 7 7 gridworld with the Moore neighbourhood and the goal in the corner state #6 and  $\beta = 100$ . A heat map showing the Decision Information, with the policy distribution denoted by arrows of length proportional to  $\beta$  (ajs) in the direction of the action, B showing the live state distribution displayed as a heat map. C provides a lookup grid with states labeled with their indices and sequence states highlighted in green. The deviation from the triangle inequality is given by  $\frac{(F_{12}(0) + F_6(12)) - F_6(0)}{F_6(0)} = 0.0005$ . We observe informationally efficient states on the diagonal, furthermore, the policy guides the agent towards these states even if it requires the agent first navigating away from the edges.

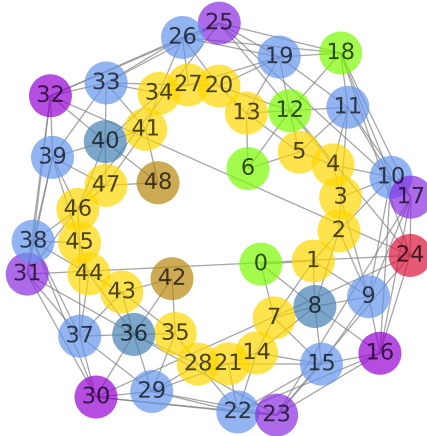
Given that corner states move closer towards each other in terms of free energy as information is increasingly more constrained, we now look at the prevalence of corner states as interim states in cost infodesics, that is, when it is expeditious to have the agent move first to a corner before continuing to the final goal. Fig. 4A and B show two near-pure infodesics for an agent with restricted information processing ( $\beta = 0.07$ ). The goal in both cases is diagonally adjacent to the middle of the grid ( $= \#18$ ). For the infodesic displayed in Fig. 4A, a starting state was arbitrarily chosen on the opposite side of the grid ( $s_0 = \#38$ ). For the second infodesic, Fig. 4B, the starting state is a nearby corner state ( $s_0 = \#0$ ). In each case it is informationally cheaper to have the agent first move into the corner adjacent to the goal ( $s^0 = 6$ ). Fig. 4B extends the infodesic to travel outwards along the central diagonal to the final goal,

$$s_0!_g = \#0; \#6; \#12; \#18$$

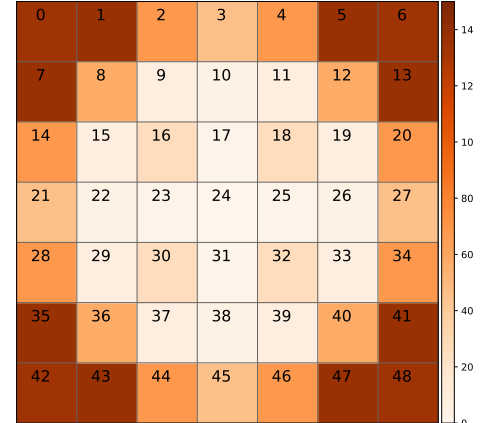
In general the agent utilises the corners as cheaper waypoints. In Fig. 4C we introduce a two-dimensional histogram in the form of a heat map which counts how often each state occurs as an interim state in an infodesic; we here consider all  $\beta$ -infodesics with  $\beta < 0.05$  of the form  $s_0!_g = \#s_0; \#s_1; \dots; \#s_T$  with non-repeating elements. The counts show that corners, edges and states on the diagonal participate particularly frequently in infodesics. The agent is guided by optimal policies to move to the best vantage point with respect to information, a position where as many states as possible are informationally closer. This is consistent with the tendency of cognitive geometry to place corner and edge states more centrally for low information processing capacities (Fig. 2B and C).



A) sequence: 38, 6, 18.



B) sequence: 0, 6, 12, 18.



C) Heatmap showing the frequency with which states occur as interim states in  $\epsilon$ -infodesics ( $\epsilon < 0.05$ )

**Figure 4. Corner states as interim states in infodesics.** The environment is a  $7 \times 7$  gridworld with a Moore neighbourhood and trade-off value  $\beta = 0.07$ . **A** sequence #38, #6, #18, with normalised free energy  $\frac{\mathcal{F}_{18}(38) - (\mathcal{F}_6(38) + \mathcal{F}_{18}(6))}{\mathcal{F}_{18}(38)} = -0.187$ . **B** #0, #6, #12, #18 with free energy  $\frac{\mathcal{F}_{18}(0) - (\mathcal{F}_6(0) + \mathcal{F}_{12}(6) + \mathcal{F}_{18}(12))}{\mathcal{F}_{18}(0)} = -0.197$ . **C** shows a heat map of the number of times a state participates as an interim state in a 3-state  $\epsilon$ -infodesic of the form  $\psi_{s_0 \rightarrow s_g} = \langle s_0 = s, s_1 = s_i, s_2 = s_g \rangle$  with  $\epsilon < 0.05$ . The cell annotations show the numbering of the states.

We now proceed with restricting information processing to the nearly open-loop policy regime,  $\beta = 0.01$  (Fig. 5). Note that one characteristic of such an open-loop scenario is to be able to reach all relevant goals with a single action distribution.

Fig. 5A shows the transition graph of the gridworld highlighting three states of the infodesic in green. The agent starts in the corner ( $S = \#0$ ) and is required to navigate to the adjacent state  $g = \#1$ . The optimal policy to reach the adjacent final goal state is represented by the arrows in Fig. 5B with Decision Information as heat map and annotations. Since the transition function is not stochastic, the low tolerance for information cost,  $\beta = 0.01$ , means that the marginal action distribution has to generalise for as many states as possible. Hence, against naive expectation, significant probability is invested into actions moving away from the goal. The policy in state  $S = \#0$  retains a chance of moving out of the corner to the goal, although it is so small it is not visible on the plot,  $\pi(\rightarrow | S = \#0) \approx 0.016$ . The informational cost arising from this small difference in action distribution is clearly indicated in Fig. 5B where  $\mathfrak{S}_D^\pi(s_0 = \#0) \sim 0.15$  bits, in contrast to the significantly lower Decision Information values in all other states.

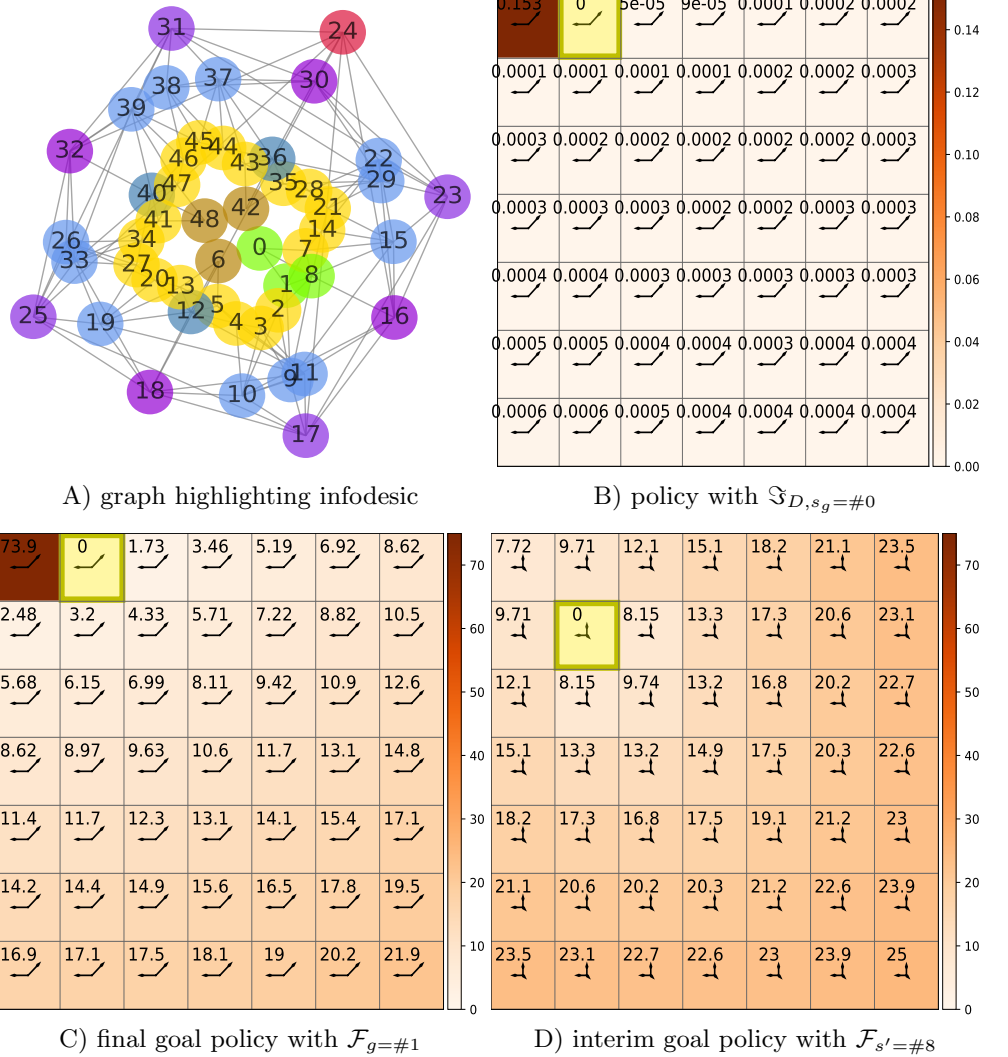
The chance that the agent successfully leaves the corner in any given time step is very low as it predominantly chooses one of the prevailing actions in the policy ( $\leftarrow$  or  $\nearrow$ ), hits the edge, pays the cost of  $-1$  in performance each time and remains in the corner without moving closer to the goal. This increased duration cost combined with the increased information cost results in a significantly higher free energy,  $\mathcal{F}_1(0) = 73.9$ , as shown in Fig. 5C which displays the same policy for the same goal ( $S = \#1$ ), but now annotated with free energy values.

It is both more performant and informationally more efficient to permit the agent to utilise an additional policy to facilitate leaving the initial corner state. To demonstrate this, we introduce an  $\epsilon$ -infodesic where the interim state is diagonally adjacent to the initial corner ( $S = \#8$ ) as shown in Fig. 5D. The agent uses one policy for the intermediate subgoal ( $s_{int} = \#8$ , policy displayed in Fig. 5D) and another policy from there to the final goal ( $g = \#1$ , displayed in Fig. 5C). This cumulative free energy, when using two policies  $\mathcal{F}_8(0) + \mathcal{F}_1(8) = 10.92$ , gives a drastic reduction of 85% in

comparison to the free energy for using a single policy,

$$\frac{\mathcal{F}_1(0) - (\mathcal{F}_8(0) + \mathcal{F}_1(8))}{\mathcal{F}_1(0)} = -0.85. \quad (12)$$

**Figure 5. Approaching open-loop policies with  $\beta = 0.01$ .**  $7 \times 7$  Moore gridworld with near-minimal information processing,  $\beta = 0.01$ . The agent starts in the corner, #0 and aims to reach the adjacent state #1. **A** Graph plot showing the  $\varepsilon$ -infodesic,  $\psi_{0 \rightarrow 1} = \langle \#0, \#8, \#1 \rangle$ , highlighted in yellow. **B** shows the policy and Decision Information for the final goal state #1 and **C** shows the same gridworld policy and goal with free energies as annotations and heatmap. **D** shows the policy and free energies for the interim goal #8.



The discussion will deal with the ramifications of introducing such switching policies.

## Discussion

When one generalises from the problem of reaching a particular goal in a cost-only MDP to a general set of goals, one makes the transition from finding optimal trajectories with a specific end state to a whole arrangement of optimal trajectories across the space. This introduces the potential of having to cater for intermittent changes of goals on the fly. More importantly, such a collection of trajectories imbues the space with additional structure, essentially a Finsler-type geometry [39] (i.e. its equivalent in the discrete case).

## Generalising Geodesics

Thinking in terms of geodesics means that instead of an optimal route between two states in the space, one can consider a starting state  $s$  and a generalised “direction”

taken from there, which in our case is reinterpreted as the choice of a policy. This means that all states on a geodesic, and not just  $g$ , are reached optimally from  $s$  under this policy. Identifying geodesics thus solves a whole class of problems at once, which is a critical motivation for the geometric perspective.

Optimal trajectories from a state  $s$  towards a goal  $g$  become a type of geodesic in this space. The Bellman property guarantees that for any intermediate state  $s'$  on such a trajectory the *remaining* part of the trajectory from  $s'$  to  $g$  must be optimal; however, for a proper interpretation as a geodesic, also the *first* part leading from  $s$  to  $s'$  should be optimal. This motivated our definition of the generalised geodesic as one where the (adapted) triangle inequality (8) holds. This generalises to any formalism which satisfies the aforementioned properties. Thus, we added information processing constraints in the form of Decision Information, generalising the pure value geodesics to *infodesics*. We have seen that this also creates characteristic distortions in the geometry of the problem under consideration and defines what we call *cognitive geometry*.

A cognitive geometry introduces some novel effects. With reduced information processing capacity, optimal policies typically become stochastic, which can render infodesics trivial, i.e. only  $s$  and  $g$  themselves fulfil the triangle inequality. We therefore included relaxed versions of the equality to still be able to consider near-infodesics. However, further, drastic deviations are possible, such as in (12), where splitting a trajectory into two parts governed by different policies can significantly *reduce* the total cost. This corresponds to switching policies at the intermediate state  $s'$  which permits the use of two different marginal action distributions throughout the run and thus enables the execution of a more complex overall policy than with a single trajectory. This reduction in information only appears because the considered triangle inequality does not include the complexity cost of a policy switchover in the Decision Information, despite this de facto requiring actual cognitive effort. We thus expect that a complete characterisation of cognitive geometry will need an expanded form of the triangle inequality that will take such policy switching costs into account.

## Free energy as a Quasimetric

To further strengthen the notion of cognitive geometry induced by the free energy formalism we have investigated whether the use of  $\mathcal{F}_g(s)$  as a distance between  $s$  and  $g$  forms a quasimetric space. This would require that free energy fulfills the following properties:

1. Nonnegativity: we have already shown that  $\mathcal{F}_g(s) \geq 0$  as  $V^\pi(s) \leq 0$  and  $\mathfrak{S}_D^\pi(s) \geq 0$ , where  $\pi$  is optimised for goal state  $g$ .
2. Principle of Indiscernibles: we know that  $\forall g \in \mathcal{G} \mathcal{F}_g(g) = 0$  as goal states are absorbing and for  $s \in \mathcal{S} \setminus g$ ,  $\mathcal{F}_g(s) \neq 0$ .
3. Asymmetry: In general, the optimal policy navigating from  $s \xrightarrow{\pi} g$  differs from the policy navigating from  $g \xrightarrow{\pi'} s$ . Therefore,  $\mathfrak{S}_D^\pi(s) \neq \mathfrak{S}_D^{\pi'}(g)$  and hence  $\mathcal{F}_g^\pi(s) \neq \mathcal{F}_s^{\pi'}(g)$  in general, making free energy at best a quasimetric.
4. Triangle inequality: we ask whether  $\mathcal{F}_g^\pi(s) \stackrel{?}{\leq} \mathcal{F}_{s'}^{\pi^{(1)}}(s) + \mathcal{F}_g^{\pi^{(2)}}(s')$ , where each segment utilises a different optimal policy  $\pi^{(1)}$  and  $\pi^{(2)}$ .

For free energy to form a quasimetric, it only remains to be shown that the triangle inequality holds. However, we have already demonstrated with a counterexample that the partitioned cumulative free energy can be lower than the free energy without subgoaling (12). Hence, in general the triangle inequality does not hold.

Maisto et al. [17] proposes that, during planning, intermediate goals are selected to minimise the computational Kolmogorov complexity. Here we propose a complementary interpretation, where making use of segmentation by incorporating interim goals reduces informational costs of the individual infodesic routes.

When segmenting an infodesic, one decomposes the original problem into subproblems with given subgoals. The constituent free energies for these subgoals utilise different policies. In the deterministic case with greedy value optimisation ( $\beta \rightarrow \infty$ ), no state will be revisited twice throughout a trajectory. This means that we can always construct a superpolicy for the overall goal-seeking behaviour by integrating the respective subpolicies. Since here there is no ambiguity about which subpolicy applies at which state, the validity of the triangle inequality for free energy is easily seen (see Supplementary Material).

Once we reduce  $\beta$ , however, the policies become increasingly stochastic to reduce the divergence from the action marginal. At some point, the stochastic trajectories belonging to different subgoals will begin overlapping en route: the agent may visit the same state during different segments of the infodesic, and therefore under different policies. At the given state it is thus now no longer uniquely resolvable without further information which of the subsegment policies is currently active. This is related to approaches enabling an agent to benefit from informationally more efficient policies which take advantage of abstractions in the environment [32, 38]. By moving to the corner opposite the goal, the agent aligns all future actions with the marginalised action distribution thereby reducing the cost of information processing even while incorporating the sequence  $\langle \#0, \#6, \#12, \#18 \rangle$ , as in Fig. 4B. This is related to epistemic actions, i.e. physical actions “that [make] mental computation easier, faster or more reliable” [12].

For a complete model of the concatenation of sub-infodesics, it would be necessary to model the detection of a subgoal being achieved, together with a memory state of the agent keeping track of the current subgoal. The informational overhead involved with the policy switching costs  $C_{switching}$  for this infodesic composition needs to be incorporated in the overall costs. Namely,  $C_{Switching}$  captures the information indicating which subgoal is currently active. Formally, we posit that while the total decision complexity is reduced by sharing the cost of information processing between multiple policies, the cost  $C_{switching}$  of maintaining these multiple policies needs to be included. We thus hypothesise a “relaxed” triangle inequality of the form:  $\mathcal{F}_g(s) \leq \mathcal{F}_{s'}(s) + \mathcal{F}_g(s') + C_{switching}$ , which, takes this switching cost into account and would be the necessary condition for using the free energy as a relaxed quasimetric. To verify and model this explicitly will be the subject of future work.

## Grid Cells and Cognitive Maps

One reason to strive towards a formalization of cognitive geometries is the long-standing idea that humans and animals form cognitive maps of their environment [36]. A large body of neurophysiological work has demonstrated that the hippocampus is sensitive to the geometry of the environment, suggesting that it may support the formation of cognitive maps [21]. Two cell types are of particular interest in this: place cells which fire at unique locations in the environment [20] and grid cells which fire at multiple locations forming a regular, triangular lattice [11]. The former is suggested to enable topological navigation while the latter may provide a spatial metric supporting path integration and vector-based navigation [6].

While there is strong evidence to suggest that the hippocampus is involved in spatial navigation, Gustafson and Daw [10] argue that the representation of location in itself may not be the sole purpose and that the hippocampal formation may instead support other important functions, such as reward-guided learning. Since success in reinforcement learning does not rely on Euclidean distance, but the distance along paths (e.g. around obstacles), the authors argue that efficient reinforcement learning should thus rely on a geodesic rather than a plain Euclidean metric. In a series of simulations, the authors provide theoretical support for the benefit and empirical evidence of this spatial coding and hypothesise that the firing of place and grid cells may be modulated accordingly.

In line with this work, we here additionally speculate that it is not only a purely geodesic metric that is of importance to biological agents, but that additional cognitive

---

costs, which we model by information-theoretical quantities, should also affect computations and hence be supported by the underlying metric. In this regard it is also worth noting that work on conceptual learning has argued that the hippocampus does not exclusively encode *spatial* properties of the environment, but that it is also involved in the representation of conceptual spaces [4, 34]. This suggests that activity of cells found in the hippocampal formation may reflect geometrical properties more generally. In this light, it appears not without reason to hypothesise that this brain area may also be a good candidate to probe for its sensitivity to the geometry that arises from a trade-off between value and information as demonstrated in this work.

## Conclusions

We considered distances induced by cost-only MDPs which were additionally endowed with an informational cost reflecting the complexity of decision-making. Geodesics generalise the intuition about geometry determined by directions and distances, representing optimal transitions between states. We proposed that the addition of informational criteria would characterise a *cognitive geometry* which additionally captures the difficulty of pursuing a particular trajectory.

We found that free energy retains some of the structure of the spatial geometry via the value function while incorporating the cost of information processing. However, emphasizing the most informationally efficient policy amongst otherwise equivalent policies will favour trajectories which pass through informationally efficient states en route to the goal. Such trajectories therefore often experience a “detour” in terms of pure distance through more easily manoeuvrable hubs. We found considerable distortions which place boundary states more centrally in the space, with the boundaries acting as guides. Additionally, when considering infodesics, i.e. sets of intermediate states which are optimally reachable from the starting state, intermediate goals can be achieved en route to the final goal, thus defining classes of problems that are solved as a side effect of solving the main one.

Analogously to geodesics, we characterised the infodesic property by the triangle inequality becoming an equality. Since this inequality is not always perfectly respected in our framework, we had to relax the conditions. Furthermore, due to the informational nature of the free energy distance, splitting a trajectory absorbs the cost of switching the policies of the two segments into the split itself and thus the violation of the triangle inequality can be quite significant. In the future, the splitting cost will be explicitly incorporated into a generalised, but tighter triangle inequality for a more stringent description of the infodesic.

Establishing such a cost, we propose, will allow us to impose, with its quasi-distance structure and additionally the “directional” structure induced by the policy choice, a quasi-geometrical signature on the state space. We suggest that this offers the basis of a genuinely geometrical notion of task spaces that takes into account cognitive processing: a cognitive geometry. This we understand to be a structure with optimal trajectories determined by either two states or by one state and a “direction” (i.e. policy) that is informed not only by the pure spatial geometry, but also by the cognitive costs that an agent needs to process when moving from task to task and how it has to informationally organise policies to achieve nearby or related tasks. Critically, such a concept would suggest that straightforward use of Euclidean, or geodesic-based geometry may not be the appropriate language to treat even purely navigational decision problems. For that reason, it would be interesting to investigate this distance further.



---

# Supporting Material

## Code Repository

All code, data (including Jupyter notebooks to reproduce the simulations) is available from the Adaptive Systems repository via <https://gitlab.com/uh-adapsys/cognitive-geometry/>.

## Information Theory

Information is described as uncertainty by Shannon, if an outcome is known, then there is no uncertainty and observing the event gives us no new information. As such, the uncertainty in  $X$  can be measured using Shannon's entropy [5]. Let  $X$  be a discrete random variable with alphabet  $\mathcal{X}$ ,  $X \in \mathcal{X}$ , and  $X \sim p(x)$ . The entropy  $H(X)$  is defined by

$$H(X) \doteq - \sum_{x \in \mathcal{X}} p(x) \log p(x). \quad (\text{i})$$

The probability mass function  $\Pr\{X = x\}$  is denoted in brief as  $p(x)$  by abuse of notation, whenever its meaning is unambiguous. Here, the logarithm is taken with respect to base 2 and information is measured in bits. We also apply the usual convention of setting  $0 \log 0 = 0$  as by continuity of  $x \log x \rightarrow 0$  for  $x \rightarrow 0$  from above.

Relative entropy, or the Kullback-Leibler divergence  $D_{KL}$  (ii), is a measure of how much additional information is processed through coding according to an assumed distribution  $q(X)$  as compared to when one would assume the correct distribution  $p(X)$ . Although it is often interpreted as a distance measure between two probability distributions, it is not a true metric between the distributions because it is not symmetric and does not satisfy the triangle inequality [5].

$$D_{KL}[p(X)||q(X)] = \sum_{x \in \mathcal{X}} p(x) \log \frac{p(x)}{q(x)}. \quad (\text{ii})$$

Extending the continuity argument above, we adopt the convention that  $0 \log \frac{0}{r} = 0$  and  $s \log \frac{s}{0} = \infty$  for all  $r \geq 0$  and  $s > 0$ .

## Value Function

A policy  $\pi(a|s)$  is a mapping between a state and action pair, and the probability of taking that action in that state, namely  $\pi : A \times S \rightarrow [0, 1]$ , in particular, for each  $s$ , summing the policy over  $a$  totals one. The policy in general defines a stochastic choice of actions. We then consider the distribution of all possible future trajectories (denoted by  $\Xi(s_0, \pi)$ ) an agent can traverse starting in  $s_0 \in \mathcal{S}$ , following the policy  $\pi$  until the trajectory terminates at a goal state  $s_T = g$ . The realisation of a particular trajectory within this distribution is denoted by  $\xi \in \Xi(s_0, \pi)$ . Throughout the paper we are dealing with optimal policies and assume that the agent ultimately reaches the goal which is absorbing. Given a fully connected world with no recurrent states, the time of termination  $T$  is a random variable which varies according to the length of the trajectory. Under the Markov assumption one has the probability:

$$p(\xi(s_0, \pi)) = p(a_0, s_1, a_1, \dots, s_T | s_0) = \prod_{t=0}^{T-1} \pi(a_t | s_t) p(s_{t+1} | s_t, a_t). \quad (\text{iii})$$

The return  $R_t$  for a sequence of actions from time  $t$  to the final time step  $T$  is the sum of the rewards for each time step [31].

$$R_t \doteq r(s_{t+1}, s_t, a_t) + r(s_{t+2}, s_{t+1}, a_{t+1}) + \dots + r(s_T, s_{T-1}, a_{T-1}). \quad (\text{iv})$$



The value function  $V^\pi(s_t)$  represents the expected return of an agent when starting in a given state  $s_t$  and following policy  $\pi$  to the end of the trajectory:

$$V^\pi(s_t) \doteq \mathbb{E}_{p(\xi)} [R_t | s_t]. \quad (\text{v})$$

Value functions define a partial ordering over policies. A policy  $\pi'$  is said to be better than or equal to another policy  $\pi$  if the value function indicates a better performance, i.e.  $V^\pi(s) \leq V^{\pi'}(s)$  for all  $s \in \mathcal{S}$ . There is always at least one value optimal policy  $\pi_V^*$  with optimal value  $V^*$  which is better or equal to all other policies. Later we talk about the policy which minimises free energy  $\pi_F^*$  which results in the agent acting optimally, but under a given information constraint specified by a trade-off parameter  $\beta$ .

## Information-to-go

*Information-to-go* (vi) quantifies the information processed by the whole agent-environment system over the course of the state-action sequences. It is the Kullback-Leibler divergence between the joint probability of future trajectories conditioned on the current state and action, and a fixed or estimated prior. It is the information required to enact the trajectory by the whole agent-environment system as compared to the prior and can be decomposed into separate components for decision complexity and for the response of the environment [35]. As a Kullback-Leibler divergence, Information-to-go is non-negative [5]:

$$\mathfrak{I}^\pi(s_t, a_t) \doteq \mathbb{E}_{p(s_{t+1}, a_{t+1}, s_{t+2}, a_{t+2}, \dots | s_t, a_t)} \left[ \log \frac{p(s_{t+1}, a_{t+1}, s_{t+2}, a_{t+2}, \dots | s_t, a_t)}{\hat{p}(s_{t+1}, a_{t+1}, s_{t+2}, a_{t+2}, \dots)} \right]. \quad (\text{vi})$$

As we are investigating geometry, to ensure that can compare distances. We thus wish to quantify the path from a given state to a target state, without, at this point, considering an initial action and therefore do not condition on the current state and action pair, but rather on the current state only. Using the linearity of expectation, the rules of logarithms and joint probabilities of independent events, we can separate the first term resulting in a Bellman-like recursive equation for Information-to-go. The expectation is again over the future trajectories originating from state  $s_t$  when following policy  $\pi$ , with the marginal distribution  $\hat{p}(a_t)$  as described in the main text, see also (3).

$$\mathfrak{I}^\pi(s_t) = \mathbb{E}_{p(\xi)} \left[ \log \frac{p(a_t, s_{t+1} | s_t)}{\hat{p}(a_t, s_{t+1})} + \log \frac{p(a_{t+1}, s_{t+2}, a_{t+3}, s_{t+4} \dots | s_{t+1})}{\hat{p}(a_{t+1}, s_{t+2}, a_{t+2}, \dots)} \right] \quad (\text{vii})$$

$$\begin{aligned} &= \sum_{p(a_t, s_{t+1} | s_t)} p(a_t, s_{t+1} | s_t) \left[ \log \frac{p(a_t, s_{t+1} | s_t)}{\hat{p}(a_t, s_{t+1})} \right. \\ &\quad \left. + \sum_{p(a_{t+1}, s_{t+2}, a_{t+2} \dots | s_{t+1})} p(a_{t+1}, s_{t+2}, a_{t+2} \dots | s_{t+1}) \log \frac{p(a_{t+1}, s_{t+2}, a_{t+3}, s_{t+4} \dots | s_{t+1})}{\hat{p}(a_{t+1}, s_{t+2}, a_{t+2}, \dots)} \right] \end{aligned} \quad (\text{viii})$$

$$= \mathbb{E}_{p(a_t, s_{t+1} | s_t)} \left[ \log \frac{\pi(a_t | s_t)}{\hat{p}(a_t)} + \log \frac{p(s_{t+1} | s_t, a_t)}{\hat{p}(s_{t+1})} + \mathfrak{I}_\pi(s_{t+1}) \right] \quad (\text{ix})$$

Modelling the decision process using the perception-action loop, we can use Information-to-go to understand the circular flow of information between the agent and the environment. Information-to-go comprises terms signifying the *environmental response* and the *decision complexity* for each state-action transition (x) [35]. The state distribution  $\hat{p}(s; \beta)$  is calculated using a live state distribution as discussed in the “Methods” section of the main text.

$$\Delta \mathfrak{I}_{s_{t+1}}^\pi(s_t) = \mathbb{E}_{\pi(a | s_t)} \left[ \log \frac{\pi(a_t | s_t)}{\hat{p}(a_t)} + \log \frac{p(s_{t+1} | s_t, a_t)}{\hat{p}(s_{t+1}; \beta)} \right]. \quad (\text{x})$$

The environmental response term,  $\log \frac{p(s_{t+1}|s_t, a_t)}{\hat{p}(s_{t+1})}$ , is the information processed by the environment for the state transition, analogous to the information gained if the agent could fully observe the successor state. This term is constant in a world with a deterministic transition model and a uniform state distribution, as a result, minimising the environmental response ensures goal directed behaviour as it essentially minimises the number of transitions.

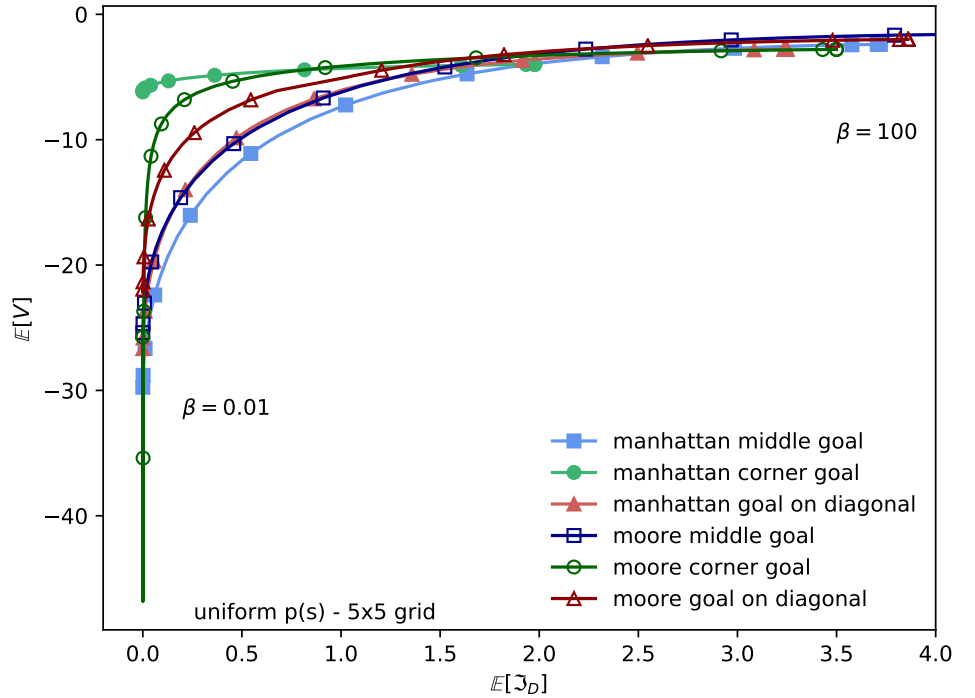
To investigate the information processed by an agent while making a decision, we define Decision Information  $\mathfrak{I}$  and by focusing on the decision complexity term,  $\log \frac{\pi(a_t|s_t)}{\hat{p}(a_t)}$ , we obtain a measure of the surprise of the agent of the future actions in the decision sequence given the prior action distribution.

$$\mathfrak{I}_D^\pi(s) \doteq \mathbb{E}_{p(a, s'|s)} \left[ \log \frac{\pi(a|s)}{\hat{p}(a)} + \mathfrak{I}_D^\pi(s') \right]. \quad (\text{xi})$$

## Cognitive Trade-off

A decision-maker may be limited by resources or may choose to act parsimoniously with respect to information processing, with a consequent reduction in performance. This trade-off between cognitive burden and performance [37] is shown in Fig. S1 by plotting behavioural performance measured by the average value function ( $\mathbb{E}_{p(s) \sim \mathcal{U}: \frac{1}{|\mathcal{S}|}} [V^\pi(s)]$ ) against the average Decision Information ( $\mathbb{E}_{p(s) \sim \mathcal{U}: \frac{1}{|\mathcal{S}|}} \sum_{s, g \in \mathcal{S}} [\mathfrak{I}_D^\pi(s)]$ ). Manhattan and Moore neighbourhoods are represented on the graph by solid and unfilled markers respectively, the shape of the marker is indicative of the goal location. Because an

**Figure S1.** Trade-off curves for Manhattan ( $\uparrow, \leftarrow, \downarrow, \rightarrow$ ) and Moore ( $\uparrow, \nearrow, \leftarrow, \swarrow, \downarrow, \searrow, \rightarrow, \nearrow$ ) neighbourhoods in a deterministic  $5 \times 5$  gridworld. Three goal states are considered: the middle, the corner of the world, and on the diagonal between the centre and the corner. Expected performance ( $\mathbb{E}[V]$ ) is plotted against expected information ( $\mathbb{E}[\mathfrak{I}_D^\pi]$ ) for various  $\beta$  values ranging from  $1 \times 10^{-3}$  to 100.



ordered set of actions is available in each state [26], corner goals are informationally cheaper to reach. In the Moore neighbourhood, an agent can take repeated actions diagonally, in the case of the Manhattan neighbourhood, the agent randomly alternates between a pair of actions to move approximately diagonally that then get additional guidance along the edges, bumping into them incurs only a minor time penalty. Thus the wall acts as a guide or “funnel” buffering some wrong actions on the way to the corner goal. In contrast, to reach the middle goal, any wrong action is likely to move the agent away from the goal. Thus much more accurate control is required to reach precisely the middle goal compared to drifting into a corner.

In our case, processing less information (low  $\beta$  values) leads to the agent being less discerning of its state and thus acting more generally, resulting in longer routes to the goal, i.e. lower values for the value function. From the graph it is clear that permitting maximal information processing permits maximising performance, and attaining the optimal value function.

## Free Energy Minimisation

To recap, we define free energy as the Lagrangian of the value function constrained by Decision Information, as detailed below and described in the main paper.

$$\mathcal{F}^\pi(s; \beta) \doteq \frac{1}{\beta} \mathfrak{S}_D^\pi(s) - V^\pi(s). \quad (\text{xii})$$

Minimising the free energy (xii) directly enables us to find the policy which achieves a particular level of performance under a constraint on information processing specified by the trade-off parameter  $\beta$ , i.e.

$$\min_{\pi(a|s)} \mathfrak{S}^\pi(s) \text{ s.t. } V^\pi(s) = \tilde{V}^\pi(s). \quad (\text{xiii})$$

Similarly to Rubin et al. [30] and further clarified by Larsson et al. [14] we proceed as described below.

For convenience, we adopt the notation  $s = s_t$ ,  $a = a_t$ ,  $s' = s_{t+1}$ , and  $r = r(s', s, a)$  and define

$$Q_{\mathcal{F}}(s, a; \beta) \doteq \sum_{s'} p(s'|s, a) (r(s', s, a) - \mathcal{F}^\pi(s'; \beta)). \quad (\text{xiv})$$

The partition function  $Z$  which is later used for normalisation of the policy is then defined in terms of the marginal of the policy as

$$Z(s; \beta) \doteq \sum_a \hat{p}(a) \exp[\beta Q_{\mathcal{F}}(s, a; \beta)], \quad (\text{xv})$$

with the marginal action distribution

$$\hat{p}(a; \pi) = \sum_{s \in \mathcal{S}} \pi(a|s) \hat{p}(s; \pi). \quad (\text{xvi})$$

Then, by taking the partial derivative of the aforementioned Lagrangian with respect to the policy, setting it to zero and solving for the policy one obtains:

$$\pi(a|s) = \frac{\hat{p}(a)}{Z(s; \beta)} \exp[\beta Q_{\mathcal{F}}(s, a; \beta)]. \quad (\text{xvii})$$

Substituting this equation for the policy into the free energy equation (6) we obtain

$$\mathcal{F}_\pi(s; \beta) = -\frac{1}{\beta} \log Z(s; \beta). \quad (\text{xviii})$$

For a fixed  $\beta \in (0, \infty)$ , we have computed the free energy optimal policy in terms of  $\hat{p}(a)$ , which itself depends on  $\pi(a|s)$ . Thus we iterate to find a solution (as detailed in algorithm 1 below). Starting with a random guess for  $\pi(a|s)$ , we update the state and action distributions, and then calculate the partition function, policy and free energy until the policy and free energy converge to within criteria  $\epsilon_\pi$  and  $\epsilon_{\mathcal{F}}$ . The corresponding Decision Information can then be calculated using the fixed-point equation (xi) and iterated until convergence.

---

**Algorithm 1** Given  $\beta$ , find free energy optimal policy  $\pi(a|s)$  and calculate  $\mathcal{F}^\pi(s; \beta)$ .

**Require:** transition dynamics  $p(s'|s, a)$ , reward function  $r(s', s, a)$ , trade-off parameter  $\beta$

Actions:  $\mathcal{A} = \{a_1, \dots, a_m\}$

States:  $\mathcal{S} = \{s_1, \dots, s_n\}$

Initialise: Free-energy function:  $\mathcal{F} \leftarrow \mathbf{0}$

Initialise: Policy to be uniformly distributed,  $\pi(a|s) \sim \mathbf{U} : \frac{1}{|\mathcal{A}|}$

**repeat**

$\mathcal{F}' \leftarrow \mathcal{F}$

$\pi' \leftarrow \pi$

update  $\hat{p}(s; \pi)$  given  $\pi(a|s)$  ▷ live distribution

$\hat{p}(a) \leftarrow \sum_s \pi(a|s) \hat{p}(s; \pi)$  ▷ marginal action distribution (xvi)

**for all**  $s \in \mathcal{S}$ ,  $a \in \mathcal{A}$ ,  $s' \in \mathcal{S} : p(s'|s, a) > 0$  **do**

$Q_{\mathcal{F}}(s, a; \beta) \leftarrow \sum_{s'} p(s'|s, a) (r(s', s, a) - \mathcal{F}'(s'; \pi, \beta))$  ▷ (xiv)

$Z(s; \beta) \leftarrow \sum_a \hat{p}(a) \exp[\beta Q_{\mathcal{F}}(s, a; \beta)]$  ▷ (xv)

$\pi(a|s) \leftarrow \frac{\hat{p}(a)}{Z(s; \beta)} \exp[\beta Q_{\mathcal{F}}(s, a; \beta)]$  ▷ (xvii)

$\mathcal{F}(s; \beta) \leftarrow -\frac{1}{\beta} \log Z(s; \beta)$  ▷ (xviii)

**until** Convergence:  $|\mathcal{F} - \mathcal{F}'| \leq \varepsilon_{\mathcal{F}}$  and  $D_{KL}[\pi || \pi'] \leq \varepsilon_{\pi}$

---

## Triangular Inequality for Disjoint Subpolicies

We show here that the free energy as a quasimetric in goal-directed navigation satisfies the triangular inequality if the trajectories produced by the subpolicies for intermediate goals never overlap (except at the subgoals themselves).

We begin with several definitions.

In the main paper we have introduced the optimal policy achieving the minimum free energy which is defined as follows:

**Definition 1** Given a goal state  $g \in S$ , define  $\pi^*$  via  $\pi^*(s) \doteq \arg \min_{\pi} \mathcal{F}_g^\pi(s)$  for all  $s \in S$ .

For this section it will be useful to define also the set of all states visited by an agent using a policy.

**Definition 2** Given a policy  $\pi$  and a state  $s \in S$ , define  $S_{\pi(s)}$  as the set containing all the states eventually visited by an agent with probability larger than 0 when starting in state  $s$  and then following the policy  $\pi$ . We include the starting state in  $S_{\pi(s)}$ , i.e.  $s \in S_{\pi(s)}$ .

In the Discussion, we have seen that, to form a proper quasi-metric on the state space  $\mathcal{S}$ , the free energy  $\mathcal{F}_g^{\pi^*}(s)$  from  $s$  to  $g$  must satisfy the following triangular inequality

$$\mathcal{F}_g^{\pi^*}(s) \leq \mathcal{F}_{s'}^{\pi^{(1)}}(s) + \mathcal{F}_g^{\pi^{(2)}}(s'), \quad (\text{xix})$$

where  $s$  is the agent's starting state,  $g$  is the goal state and  $s'$  any interim subgoal. The optimal policy  $\pi^*$  directly brings the agent from  $s$  to  $g$  without constraining possible interim states. In contrast, when composing the optimal subpolicies  $\pi^{(1)}$  and  $\pi^{(2)}$ , the agent firstly moves from  $s$  to  $s'$  (using  $\pi^{(1)}$ ) and then moves from  $s'$  to  $g$  (via  $\pi^{(2)}$ ). We remind the reader that underlying the individual free energy terms in (xix) there are actually distinct MDPs (in our formalism goals are modelled as absorbing states, see main text for details); we then hierarchically combine when considering the composition of the two terms in the right hand side of the inequality. We have already shown with a counterexample that the triangular inequality (xix), in its general form, does not hold (main text, equation (12)). In this section, we prove the triangular inequality when the subpolicies are *essentially disjoint*, i.e., if starting at  $s$ , the trajectories induced by  $\pi^{(1)}$  and those by  $\pi^{(2)}$  only intersect trivially at  $s'$  (namely, in

the case of  $\pi^{(1)}$  as goal of the first policy, in the case of  $\pi^{(2)}$  as starting state of the second policy.)

We proceed now by proving the following theorem:

**Theorem 1** *Let  $s \neq g$ ,  $s, g \in S$  be given. Then, if for all  $s' \in S$  we have  $S_{\pi^{(1)}(s)} \cap S_{\pi^{(2)}(s')} = \{s'\}$ , then  $\mathcal{F}_g^{\pi^*}(s) \leq \mathcal{F}_{s'}^{\pi^{(1)}}(s) + \mathcal{F}_g^{\pi^{(2)}}(s')$*

**Proof** For  $s' = g$  the theorem can be easily proven, since we have  $\mathcal{F}_g(g) = 0$ , then  $\mathcal{F}_g^{\pi^*}(s) = \mathcal{F}_{s'}^{\pi^{(1)}}(s) + 0 = \mathcal{F}_g^{\pi^{(1)}}(s)$ , which fulfils the triangular inequality, and analogously for  $s' = s$ . Therefore, assume  $s \neq s' \neq g$  and we employ proof by contradiction. We will show that, if there exists a  $s' \neq g$  violating this condition (i.e. for which the inequality is reversed and strict), then we can glue the subpolicies  $\pi^{(1)}$  and  $\pi^{(2)}$  together in a way such that the resulting new policy  $\hat{\pi}^*$  achieves a smaller overall free energy than the original optimal policy  $\pi^*$ , leading to a contradiction.

Formally, assume that there exists  $s' \in S$ , with  $s' \neq g$ , for which  $\mathcal{F}_g^{\pi^*}(s) > \mathcal{F}_{s'}^{\pi^{(1)}}(s) + \mathcal{F}_g^{\pi^{(2)}}(s')$ . Then, construct a new policy  $\hat{\pi}^*$ , via:

$$\forall q \in \mathcal{S}: \quad \hat{\pi}^*(a|q) \doteq \begin{cases} \pi^{(1)}(a|q) & \text{if } q \in S_{\pi^{(1)}(s)} \setminus \{s'\} \\ \pi^{(2)}(a|q) & \text{if } q \in S_{\pi^{(2)}(s')} \end{cases}$$

Note that, similar to  $\pi^*$ , also  $\hat{\pi}^*$  can be used by an agent to reach the goal  $g$  from the initial state  $s$ . Furthermore, since we assumed  $S_{\pi^{(1)}(s)} \cap S_{\pi^{(2)}(s')} = \{s'\}$ ,  $\hat{\pi}^*$  is well defined for each state on the possible trajectories, with no ambiguity as to which subpolicy is to be used. We can then compute the free energy  $\mathcal{F}_g^{\hat{\pi}^*}(s)$  as follows (superscripts indicate whether states and actions belong to the first or second section of the trajectory):

$$\begin{aligned} \mathcal{F}_g^{\hat{\pi}^*}(s) &= \sum_{(a_0^1, s_1^1, a_1^1, \dots, s', a_0^2, s_1^2, a_1^2, \dots, g|s)} p(a_0^1, s_1^1, a_1^1, \dots, s', a_0^2, s_1^2, a_1^2, \dots, g|s) \cdot \\ &\cdot \left( \frac{1}{\beta} \log \frac{\hat{\pi}^*(a_0^1|s)}{\hat{p}(a_0^1)} - r(s_1^1, s, a_0^1) + \frac{1}{\beta} \log \frac{\hat{\pi}^*(a_1^1|s_1^1)}{\hat{p}(a_1^1)} - \dots \right. \\ &\left. \dots + \frac{1}{\beta} \log \frac{\hat{\pi}^*(a_0^2|s')}{\hat{p}(a_0^2)} - r(s_1^2, s', a_0^2) + \frac{1}{\beta} \log \frac{\hat{\pi}^*(a_1^2|s_1^2)}{\hat{p}(a_1^2)} - \dots \right) = \\ &= \sum_{(a_0^1, s_1^1, a_1^1, \dots, s', a_0^2, s_1^2, a_1^2, \dots, g|s)} p(a_0^1, s_1^1, a_1^1, \dots, s', a_0^2, s_1^2, a_1^2, \dots, g|s) \cdot \\ &\cdot \left( \frac{1}{\beta} \log \frac{\pi^{(1)}(a_0^1|s)}{\hat{p}(a_0^1)} - r(s_1^1, s, a_0^1) + \frac{1}{\beta} \log \frac{\pi^{(1)}(a_1^1|s_1^1)}{\hat{p}(a_1^1)} - \dots \right. \\ &\left. \dots + \frac{1}{\beta} \log \frac{\pi^{(2)}(a_0^2|s')}{\hat{p}(a_0^2)} - r(s_1^2, s', a_0^2) + \frac{1}{\beta} \log \frac{\pi^{(2)}(a_1^2|s_1^2)}{\hat{p}(a_1^2)} - \dots \right), \end{aligned} \tag{xx}$$

where in the last equation we substituted  $\hat{\pi}^*$  by  $\pi^{(1)}$  or  $\pi^{(2)}$  as per the definition of  $\hat{\pi}^*$ . Now, we can use the linearity of the expected value, split the sum in (xx) and marginalizing away the superfluous variables to obtain the individual free energies

$\mathcal{F}_{s'}^{\pi^{(1)}}(s)$  and  $\mathcal{F}_g^{\pi^{(2)}}(s')$ ,

$$\begin{aligned} \mathcal{F}_g^{\hat{\pi}^*}(s) &= \\ &= \underbrace{\sum_{(a_0^1, s_1^1, a_1^1, \dots, s'|s)} p(a_0^1, s_1^1, a_1^1, \dots, s'|s) \left( \frac{1}{\beta} \log \frac{\pi^{(1)}(a_0^1|s)}{\hat{p}(a_0^1)} - r(s_1^1, s, a_0^1) + \frac{1}{\beta} \log \frac{\pi^{(1)}(a_1^1|s_1^1)}{\hat{p}(a_1^1)} - \dots \right)}_{\mathcal{F}_{s'}^{\pi^{(1)}}(s)} + \\ &\quad \underbrace{\sum_{(a_0^2, s_1^2, a_1^2, \dots, g|s')} p(a_0^2, s_1^2, a_1^2, \dots, g|s') \left( \frac{1}{\beta} \log \frac{\pi^{(2)}(a_0^2|s')}{\hat{p}(a_0^2)} - r(s_1^2, s', a_0^2) + \frac{1}{\beta} \log \frac{\pi^{(2)}(a_1^2|s_1^2)}{\hat{p}(a_1^2)} - \dots \right)}_{\mathcal{F}_g^{\pi^{(2)}}(s')} = \end{aligned}$$

$$\mathcal{F}_{s'}^{\pi^{(1)}}(s) + \mathcal{F}_g^{\pi^{(2)}}(s') < \mathcal{F}_g^{\hat{\pi}^*}(s),$$

(xxi)

The last inequality directly comes from our main assumption of violating the triangular inequality. In equation (xxi) we have proven that  $\mathcal{F}_g^{\hat{\pi}^*}(s) < \mathcal{F}_g^{\pi^*}(s)$ ; i.e. when moving from  $s$  to  $g$  via  $s'$  and the composite policy  $\hat{\pi}^*$ , the free energy is smaller than the free energy obtained using  $\pi^*$ . But  $\pi^*$  was assumed optimal, hence the assumption that the triangle inequality is violated leads to a contradiction. It therefore must hold and the proof is established.  $\square$

## References

1. R. E. Blahut. Computation of Channel Capacity and Rate-Distortion Functions. *IEEE Transactions on Information Theory*, 18(4):460–473, 1972.
2. N. Catenacci Volpi and D. Polani. Space emerges from what we know—spatial categorisations induced by information constraints. *Entropy*, 22(10):1179, 2020.
3. N. Catenacci Volpi and D. Polani. Goal-directed empowerment: Combining intrinsic motivation and task-oriented behaviour. *IEEE Transactions on Cognitive and Developmental Systems*, 2020.
4. A. O. Constantinescu, J. X. O’Reilly, and T. E. Behrens. Organizing conceptual knowledge in humans with a gridlike code. *Science*, 352(6292):1464–1468, 2016.
5. T. M. Cover and J. A. Thomas. *Elements of information theory*. John Wiley & Sons Inc, New York, 2nd edition, 2006.
6. V. Edvardsen, A. Bicanski, and N. Burgess. Navigating with grid and place cells in cluttered environments. *Hippocampus*, 30(3):220–232, 2020.
7. K. Friston. The free-energy principle: A unified brain theory? *Nature Reviews Neuroscience*, 11(2):127–138, 2010.
8. T. Genewein, F. Leibfried, J. Grau-Moya, and D. A. Braun. Bounded Rationality, Abstraction, and Hierarchical Decision-Making: An Information-Theoretic Optimality Principle. *Frontiers in Robotics and AI*, 2, 2015.
9. J. Grau-Moya, F. Leibfried, and P. Vrancx. Soft Q-learning with Mutual-Information regularization. In *ICLR*, 2019.
10. N. J. Gustafson and N. D. Daw. Grid cells, place cells, and geodesic generalization for spatial reinforcement learning. *PLoS Comput Biol*, 7(10), 2011.
11. T. Hafting, M. Fyhn, S. Molden, M.-B. B. Moser, and E. I. Moser. Microstructure of a spatial map in the entorhinal cortex. *Nature*, 436(7052):801–806, 2005.

- 
12. D. Kirsh and P. Maglio. On distinguishing epistemic from pragmatic action. *Cognitive Science*, 18(4):513–549, 1994.
  13. J. B. Kruskal and M. Wish. *Multidimensional scaling*. Sage Publications, 1978.
  14. D. T. Larsson, D. A. Braun, and P. Tsiotras. Hierarchical State Abstractions for Decision-Making Problems with Computational Constraints. In *2017 IEEE 56th Annual Conference on Decision and Control (CDC)*, volume 1710.07990, 2017.
  15. F. Leibfried and J. Grau-Moya. Mutual-Information Regularization in Markov Decision Processes and Actor-Critic Learning. In *3rd Conference on Robot Learning (CoRL)*, 2019.
  16. C. Liu, X. Xu, and D. Hu. Multiobjective reinforcement learning: A comprehensive overview. *IEEE Transactions on Systems, Man, and Cybernetics: Systems*, 45(3):385–398, 2014.
  17. D. Maisto, F. Donnarumma, and G. Pezzulo. Divide et impera: Subgoalng reduces the complexity of probabilistic inference and problem solving. *Journal of the Royal Society Interface*, 12(104), 2015.
  18. S. E. Marzen and S. Dedeo. The evolution of lossy compression. *Journal of the Royal Society Interface*, 14(130), 2017.
  19. S. K. Mitter and N. J. Newton. A Variational Approach to Nonlinear Estimation. *SIAM J. Control Optim.*, 42(5):1813–1833, 2003.
  20. J. O’Keefe and J. Dostrovsky. The hippocampus as a spatial map: Preliminary evidence from unit activity in the freely-moving rat. *Brain research*, 1971.
  21. J. O’Keefe and L. Nadel. *The hippocampus as a cognitive map*. Oxford: Clarendon Press, 1978.
  22. P. A. Ortega and D. A. Braun. Thermodynamics as a theory of decision-making with information-processing costs. *Proceedings of the Royal Society A: Mathematical, Physical and Engineering Sciences*, 469(2153), 2013.
  23. P. A. Ortega, D. A. Braun, J. Dyer, K.-E. Kim, and N. Tishby. Information-Theoretic Bounded Rationality. *ArXiv*, 1512.06789, dec 2015.
  24. F. Pedregosa, G. Varoquaux, A. Gramfort, V. Michel, B. Thirion, O. Grisel, M. Blondel, P. Prettenhofer, R. Weiss, V. Dubourg, J. Vanderplas, A. Passos, D. Cournapeau, M. Brucher, M. Perrot, and E. Duchesnay. Scikit-learn: Machine Learning in Python. *Journal of Machine Learning Research*, 12:2825–2830, 2011.
  25. D. Polani. Information: currency of life? *HFSP Journal*, 3(5):307–316, 2009.
  26. D. Polani. An informational perspective on how the embodiment can relieve cognitive burden. *2011 IEEE Symposium on Artificial Life*, 2011.
  27. D. Polani, C. L. Nehaniv, T. Martinetz, and J. T. Kim. Relevant Information in Optimized Persistence vs . Progeny Strategies. In *Artificial Life X : Proceedings of the Tenth International Conference on the Simulation and Synthesis of Living*, pages 237–343. MIT Press, 2006.
  28. A. Pressley. *Elementary Differential Geometry*. Springer-Verlag, London, 2nd edition, 2010.
  29. M. L. Puterman. *Markov Decision Processes - Discrete stochastic dynamic programming*. Wiley-Interscience, 1994.

- 
30. J. Rubin, O. Shamir, and N. Tishby. Trading Value and Information in MDPs. In W. D. Guy T.V., Kárný M., editor, *Decision Making with Imperfect Decision Makers. Intelligent Systems Reference Library, vol 28*. Springer, 2012.
  31. R. S. Sutton and A. G. Barto. *Reinforcement Learning: An Introduction*. MIT Press, Cambridge MA, 2nd edition, 2018.
  32. R. S. Sutton, o. Precup, and S. Singh. Between MDPs and semi-MDPs: A framework for temporal abstraction in reinforcement learning. *Artificial Intelligence*, 112:181–211, 1999.
  33. M. E. Taylor and P. Stone. Transfer learning for reinforcement learning domains: A survey. *Journal of Machine Learning Research*, 10(7), 2009.
  34. S. Theves, G. Fernández, and C. F. Doeller. The hippocampus maps concept space, not feature space. *Journal of Neuroscience*, 2020.
  35. N. Tishby and D. Polani. Information Theory of Decisions and Actions. *Perception-Action Cycle*, pages 601–636, 2011.
  36. E. C. Tolman. Cognitive maps in rats and men. *Psychological review*, 55(4):189, 1948.
  37. S. G. van Dijk. *Informational Constraints and Organisation of Behaviour*. PhD thesis, University of Hertfordshire, 2013.
  38. S. G. Van Dijk and D. Polani. Grounding subgoals in information transitions. In *IEEE Symposium on Adaptive Dynamic Programming and Reinforcement Learning*, pages 105–111, 2011.
  39. G. R. Wilkens. Finsler geometry in low dimensional control theory. In D. Bao, S.-S. Chern, and Z. Shen, editors, *Joint Summer Research Conference on Finsler Geometry*. American Mathematical Society, 1995.
  40. R. Yang, X. Sun, and K. Narasimhan. A generalized algorithm for multi-objective reinforcement learning and policy adaptation. *Advances in Neural Information Processing Systems*, 32, 2019.